ELSEVIER

Journal of Nuclear Materials 290–293 (2001) 829–835

journal of nuclear materials

www.elsevier.nl/locate/jnucmat

Electric fields and currents in an island divertor configuration

X. Bonnin [a,*], R. Schneider [a], D. Coster [b], V. Rozhansky [c], S. Voskoboynikov [c]

[a] *Max-Planck-Institut für Plasmaphysik, Teilinstitut Greifswald, Wendelsteinstraße, 1, EURATOM-Association, Greifswald, D-17491 Germany*

[b] *Max-Planck-Institut für Plasmaphysik, EURATOM-Association, Garching, D-85748 Germany*

[c] *St. Petersburg State Technical University, St. Petersburg, 195251 Russian Federation*

Abstract

One candidate for an optimized particle and energy exhaust concept in stellarators is the island divertor. Due to the special topology of such a design, its physics characteristics can be quite different from standard tokamak divertors or Limited Stellarator Plasmas. We have extended the capabilities of the two-dimensional B2-solps5.0 multifluid Scrape-Off layer plasma simulation code to handle diverted island geometries, including all relevant physics, in particular drifts and currents. We focus here on the structure of the electric potential and electric field in this island configuration. We show the establishment of potential and current flow patterns favoring density accumulation inside the island. This electric potential distribution is non-trivial and quite different from the $\phi = 3kT$ ansatz used in previous studies.

Keywords: Island divertor; Stellarator; Edge modelling

1. Introduction

Current (CHS, W7-AS) and future (W7-X) stellarators are being built with so-called 'island divertors' [1,2], where the divertor plates intersect magnetic islands situated at the edge of the plasma. This leads to unique geometrical features: as one moves away from the center of the island, one first encounters closed field lines, then open lines ending at the divertor plates, and finally closed lines again in the plasma core region. The presence of these two spatially separated closed field lines regions makes the physics characteristics of island divertors quite different from more conventional plasma–wall interaction regions.

In this paper, we present a study of the island divertor concept, as envisioned in W7-AS and W7-X, using the B2-solps5.0 Scrape-Off Layer Plasma Simulation code. Since the code is two-dimensional, the magnetic geometry is represented by a toroidally averaged grid [3]. This 2D ansatz forces us to restrict our analysis mostly to the structure of the electric potential and electric field, concentrating on the impact of the topological features of the island divertor, without attempting a detailed engineering study. In itself, the island divertor already constitutes an interesting system for investigating terms driving radial transport and the establishment of potential gradients.

In practice, we solve the usual set of fluid conservation equations (particles, momentum and energy) as well as the electric potential equation (in the form of the current continuity equation: $\nabla \cdot \mathbf{J} = 0$). The full set of equations and solution method have been described elsewhere [4,5]. Of special interest here, beyond the addition of the electric potential equation, are the diamagnetic and parallel viscosity terms, as well as the $\mathbf{E} \times \mathbf{B}$ drift, none of which were included in the previous island divertor simulations [2,6,7]. A neutral fluid model accounts for recycling and ionization effects. A more accurate representation of the neutrals would require a 3D simulation because of the complex plasma geometry. Although full 3D models of stellarator plasma edge transport are becoming available [8,9], they do not yet treat self-consistently the electric potential, or contain

* Corresponding author. Tel.: +49-03834 882416; fax: +49-03834 882409.

E-mail address: xpb@ipp.mpg.de (X. Bonnin).

0022-3115/01/$ - see front matter
PII: S0022-3115(00)00646-2

drifts and currents [7]. It is thus useful to obtain knowledge about the electric field structure of island divertors using our current 2D tokamak simulation tools. We begin by presenting the results of simulations involving no drift terms, so as to establish a reference case. Diamagnetic and parallel viscosity terms are then added, and their influence described. Finally, we discuss the further impact of the $\mathbf{E} \times \mathbf{B}$ terms.

2. The plasma edge in the presence of a diverted island

First, let us detail the geometry of the island divertor (cf. Fig. 1). For the purposes of our simulations, we use a toroidally averaged grid computed from a W7-AS equilibrium [3] with an $m/n = 5/9$ diverted island chain [2,6]. Since we restrict ourselves to a general study of the drift effects in island divertors, specific details of the individual W7-AS or W7-X islands can be neglected. In the figure, the wall is the top edge of the simulation domain, and the interface with the core is the bottom boundary. In the poloidal direction, we use periodic boundary conditions, where computational cells on the left edge of the domain are assumed to be neighboring those on the right edge of the domain.

The dominating feature of these plasma configurations is particle accumulation inside the island [2]. In that sense, the island divertor behaves very differently from a standard tokamak divertor. We show the density distribution for a typical high-recycling case in Figs. 1 and 2. A density 'pillow' across the island and SOL regions is readily apparent. For this run, we have chosen $n_e^{core} = 10^{20}$ m^{-3} and a heat flux through the core boundary of 220 kW as our boundary conditions (corresponding to 1.1 MW of SOL power influx for the complete five-island system in W7-X). Out of these 220 kW, only about 20 kW reach the plates, and the remaining 200 kW are lost to radiation and ionization of

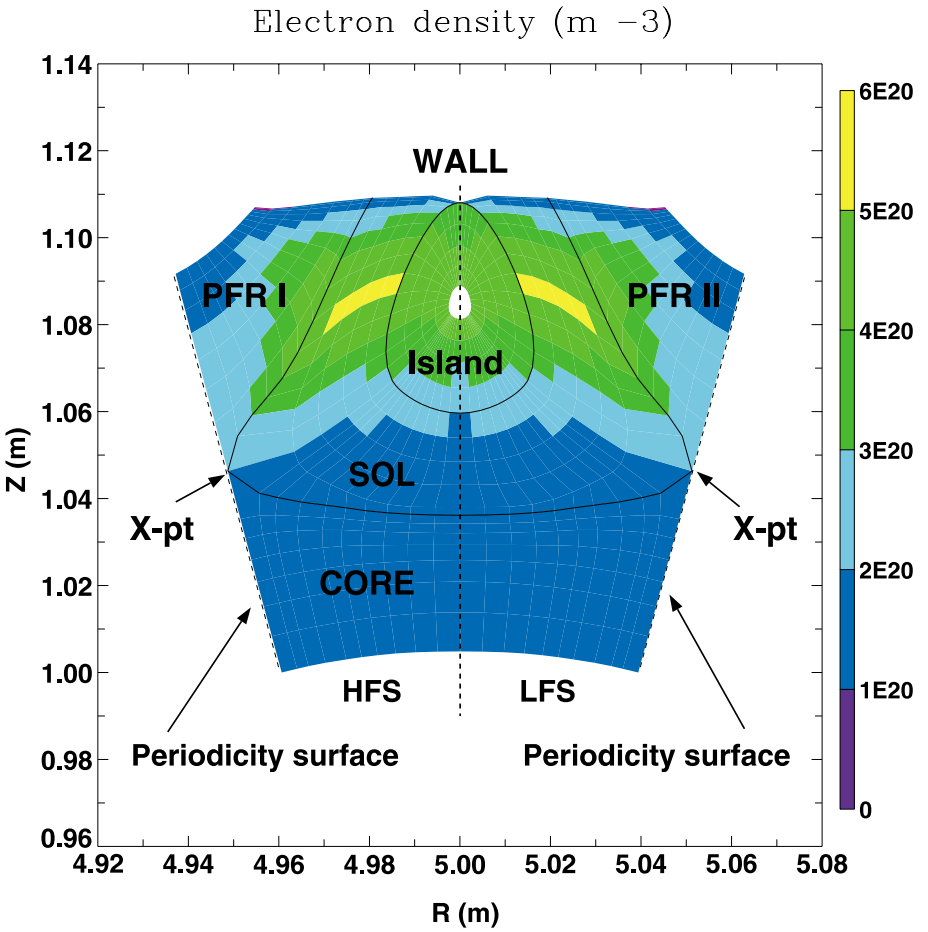

Fig. 1. Typical density distribution obtained for a no-drifts high-recycling case. The island, core, SOL and private flux regions (PFR I and II), their boundaries, X-points and periodicity surfaces are also shown. The dashed line shows the cut used for the 1D profiles in Figs. 2 and 5. HFS: High-field side; LFS: Low-field side.

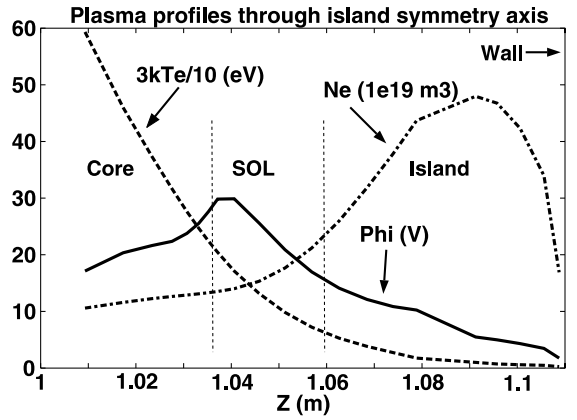

Fig. 2. Temperature (dashed line), density (dot-dashed line) and electric potential (solid line) profiles for the case shown in Fig. 1. The profiles are taken along the symmetry line at $R = 5.00$ m (dashed line in Fig. 1). Note the clear potential maximum just outside the separatrix, the density accumulation inside the island and the scale difference between 3 kT_e and ϕ.

the recycled neutrals, of which 50 kW are dissipated inside the island region. Analysis of the particle flows shows that many recycled neutrals penetrate into the island and are ionized there, thus creating a density increase in and about the island region. As can be seen in Figs. 2 and 3, the potential profile favors this density distribution by adopting a maximum near the separatrix and in general being very different from the values given by the simple $\phi = 3kT$ ansatz. Concurrently (cf. Fig. 4), current loops get established which interconnect the SOL and the island region, but do not cross into the core plasma. Mirroring current flow loops also exist in both the core and the side private flux regions. As explained in [2], the 'pillow' density depends strongly on the recycling conditions (in Figs. 1–4 we use a 99% recycling coefficient). Since the true geometry of the island is 3D and the plates are not toroidally continuous, our 2D simulations (with toroidally continuous plates) will overestimate the density accumulation. When we correct this overestimation by lowering the

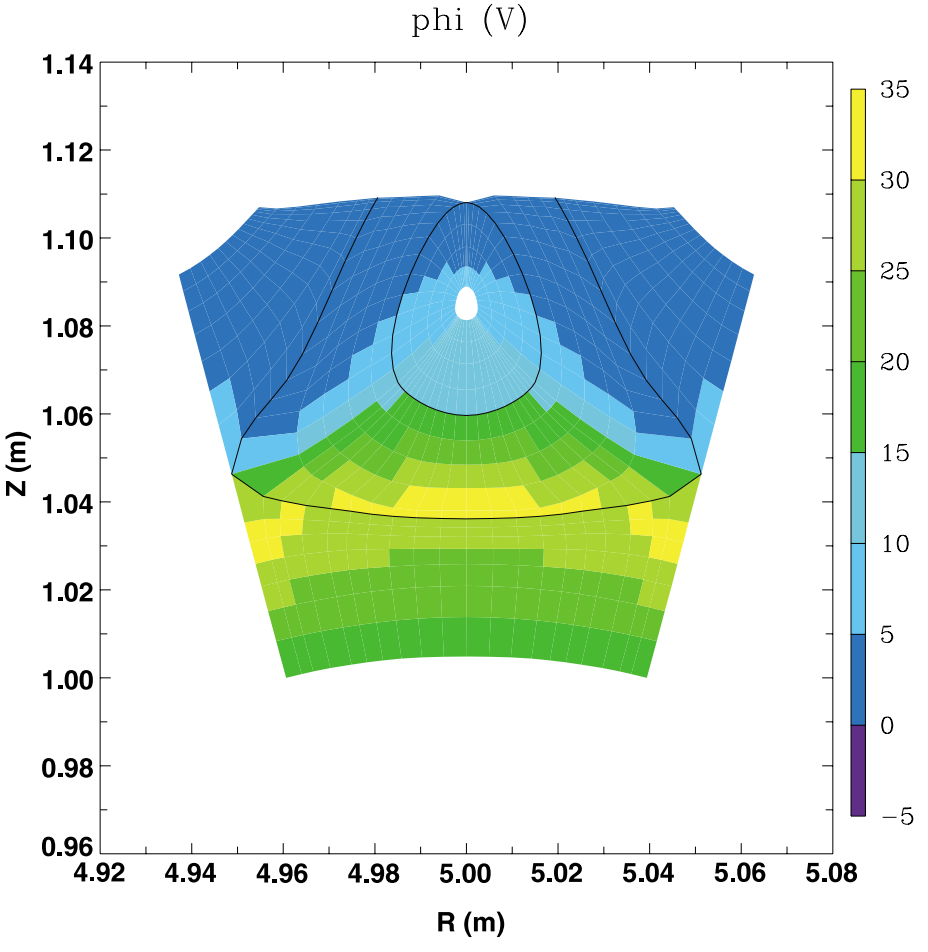

Fig. 3. Electric potential distribution for the case shown in Fig. 1.

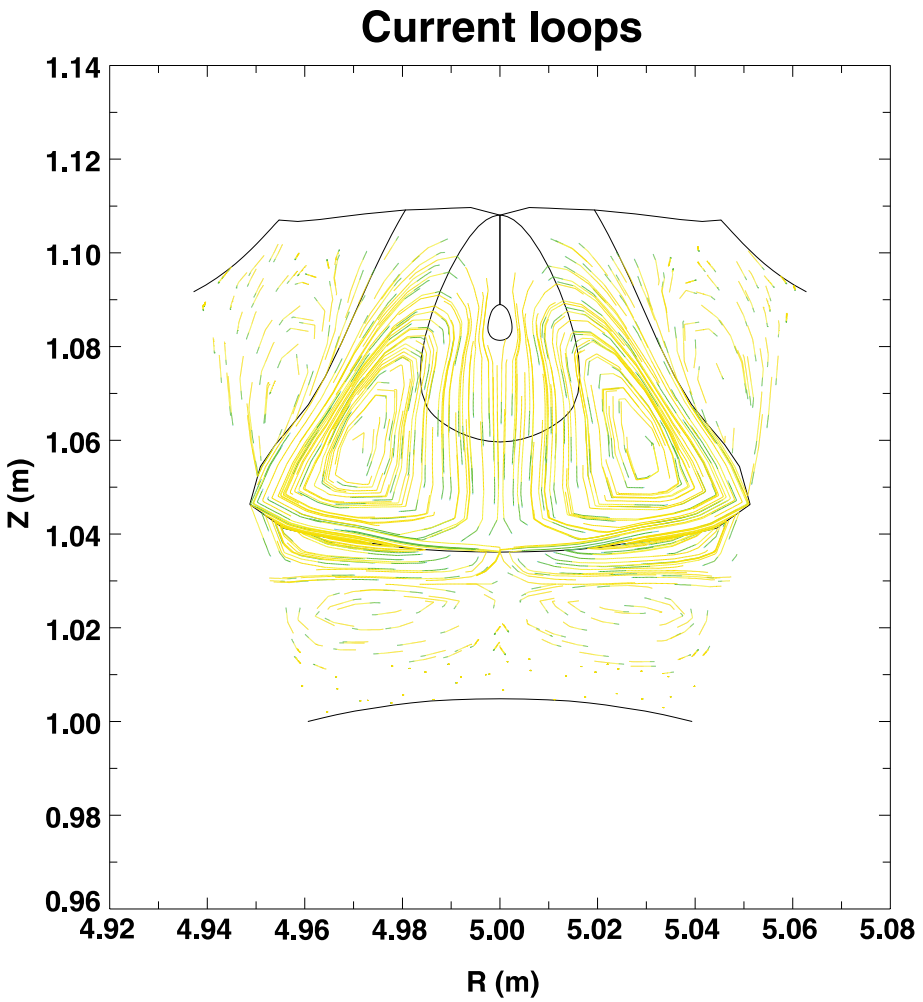

Fig. 4. Test charge trajectories illustrating the current flow loops present in the plasma for the case shown in Fig. 1.

recycling coefficient, the island density accumulation rapidly disappears, while the current loops in the SOL become narrower, eventually failing to cross over into the island region.

3. Influence of diamagnetic and parallel viscosity terms

We now proceed up in complexity in our model plasma description by including parallel viscosity and diamagnetic terms, restricting ourselves for simplicity to the single ion species plasma case [4]. The x and y directions correspond to directions along and across flux surfaces, respectively. The metric coefficients are $h_x = 1/\|\nabla x\|$ and $h_y = 1/\|\nabla y\|$. The subscript $\perp$ denotes the direction perpendicular to both the magnetic field $\vec{B}$ and the y-axis. The magnetic field unit vector components are denoted as $b_x = B_x/B$, etc.

Normally, the perpendicular current is modeled using an anomalous cross-field conductivity. The addition of parallel viscosity implies a perpendicular current term of the following form, after its divergence-free component has been removed

$$\tilde{j}_{\perp}^{(\mathrm{vis}\|)} = -\frac{B_x \eta_0}{3\sqrt{B}} \frac{\partial (V_\| \sqrt{B})}{h_x \partial x} \frac{\partial}{h_y \partial y}\left(\frac{1}{B^2}\right), \tag{1}$$

where $\eta_0 = 0.96 n T_i / \nu_{ii}$ is the parallel viscosity coefficient. However, the largest contribution to the non-divergence-free perpendicular current comes from the diamagnetic term

$$\tilde{j}_{\perp}^{(\mathrm{dia})} = \frac{1}{b_z} \frac{n(T_e + T_i) B_z}{h_y} \frac{\partial}{\partial y}\left(\frac{1}{B^2}\right). \tag{2}$$

The other influences of the diamagnetic drift are an effective cross-field velocity

$$\tilde{V}_{\perp}^{(\mathrm{dia})} = \frac{T_i B_z}{e b_z} \frac{\partial}{h_y \partial y}\left(\frac{1}{B^2}\right), \tag{3}$$

and a heat flux term, often referred to as the $\nabla T \times \mathbf{B}$ term, whose non-divergence-free components can be expressed as

$$\tilde{q}_{ex}^{(\mathrm{dia})} = -\frac{5}{2} n T_e^2 \frac{B_z}{e} \frac{\partial}{h_y \partial y}\left(\frac{1}{B^2}\right), \tag{4a}$$

$$\tilde{q}_{ey}^{(\mathrm{dia})} = +\frac{5}{2} n T_e^2 \frac{B_z}{e} \frac{\partial}{h_x \partial x}\left(\frac{1}{B^2}\right). \tag{4b}$$

Whether one deals with the diamagnetic or $\mathbf{E} \times \mathbf{B}$ perpendicular drift velocity, special care must be taken to avoid unphysical flows at the plates. The standard boundary condition is to require that the flow be at least sonic at the sheath entrance [10], which translates into:

$$V_{\parallel} \geqslant C_s - \frac{b_z}{b_x} V_{\perp}, \tag{5}$$

where C_s is the local sound speed and b_z/b_x is the inverse of the field line pitch. However, for very small pitch angles, as in stellarators, the $V_{\perp}$ term may overpower the sound velocity [8] and then the boundary condition would require a plasma flow exiting the plate. Therefore, we have limited the pitch angle at the plates to be not less than one degree, motivated by the engineering limits met when attempting to align the divertor tiles with the magnetic field. The solution procedure of the code was also modified so as ensure that no unphysical flows were being created, and solves the parallel momemtum equation using the updated electric potential. The formalism used for the core boundary conditions, which assumes closed field lines and balances diamagnetic and parallel viscosity currents [4], has been generalized to handle the island center boundary as well. Lastly, the toroidal averaging algorithm [3] gives divergent values for the magnetic field strength (but not for the pitch angle) along the island symmetry axis. Hence, the values of B_z and B_x were modified ($B_y = 0$ by construction) so that (1) the magnitude of B match that expected in the divertor region of W7-X and (2) the field line pitch B_x/B_z remain the same as in the toroidally averaged grid (thus keeping the connection lengths unchanged). Since B is then no longer toroidally averaged in an absolute sense, it loses its strict periodicity. We thus avoid computing the derivatives of $1/B^2$ across the periodicity boundary by using face-centered values for the field components in cells next to that boundary.

The main consequence of the inclusion of the diamagnetic terms is the establishment of very strong radial potential gradients in the core region, fundamentally altering the electric field structure (see Fig. 5). These gradients destroy the current loops that were previously connecting the SOL and diverted island regions and thus wash away most of the density inversion seen in the no-drifts case, with only the center of the island still maintaining a slight density enhancement, as ionization of recycled neutrals still takes place in this region. Most of the current now flows in a semi-vertical pattern (in our geometry): from the plates, around the island, radially drifting towards the separatrix and once inside the core plasma almost purely radially. This behavior is similar to what has been seen for tokamak cases [11]. The diamagnetic and parallel viscosity currents replace the anomalous perpendicular current (used for numerical stability reasons) of the no-drifts runs. As that numerical ansatz is relaxed, the potential gradient increases, roughly as the inverse of the anomalous perpendicular conductivity.

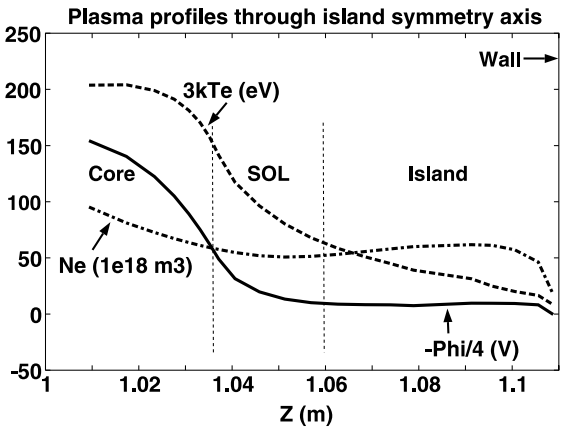

Fig. 5. Same as Fig. 2, but with diamagnetic and parallel viscosity effects included. Note the shallow density build-up inside the island and the change of scales for all three quantities. The electric potential had its sign changed for clarity of presentation.

4. $\mathbf{E} \times \mathbf{B}$ effects

In this section, we add to the simulations the $\mathbf{E} \times \mathbf{B}$ velocity:

$$\mathbf{v}_{\mathbf{E}\times\mathbf{B}} = \frac{\mathbf{B} \times \nabla \Phi}{\mathbf{B}^2}, \tag{6}$$

as well as the related heating source term

$$Q_{e,i}^{\mathbf{E}\times\mathbf{B}} = n T_{e,i} B \frac{1}{h_x h_y}\left(\frac{\partial \Phi}{\partial y}\frac{\partial}{\partial x}\left(\frac{1}{B^2}\right) - \frac{\partial \Phi}{\partial x}\frac{\partial}{\partial y}\left(\frac{1}{B^2}\right)\right). \tag{7}$$

From a numerical point of view, those terms are more difficult to include. In particular, the potential and momentum equations are coupled non-linearly by the $\mathbf{E} \times \mathbf{B}$ velocity terms. This effect is most serious at the divertor plates, as discussed in Section 3. Applying only the $\mathbf{E} \times \mathbf{B}$ terms, without their diamagnetic counter-

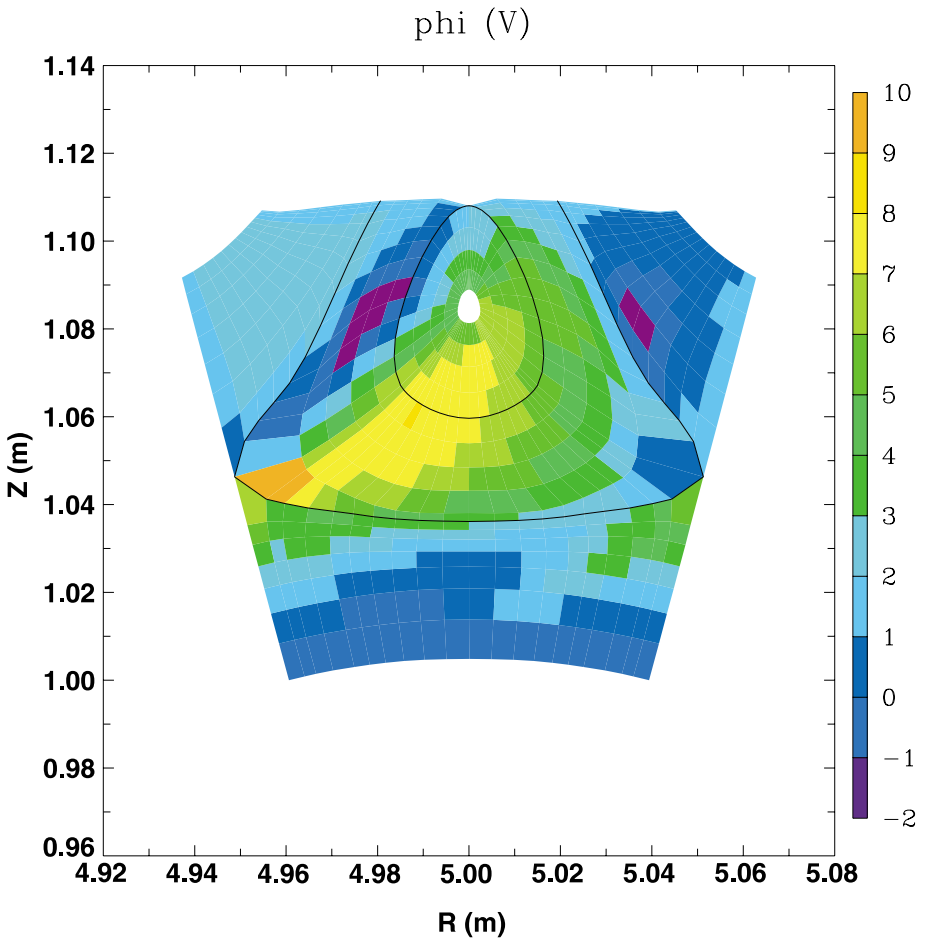

Fig. 6. Same as Fig. 3, but with $\mathbf{E} \times \mathbf{B}$ drift included.

parts, one sees, as expected, a large imbalance between the two sides of the SOL region. For our geometry, it is the high-field side of the SOL that experiences a density enhancement and where the potential minimum resides, although the actual values of the potential remain small. As seen in Fig. 6, the region of maximum potential forms an asymmetrical ridge going from the high-field side X-point to the island center, falling off rapidly towards the inner divertor plate, and much more slowly in the opposite poloidal direction. The current loops have been strongly deformed, the high-field side loops elongating and swallowing most of the low-field side structures, while the core current becomes mostly poloidal.

The most challenging step is of course to turn on both the diamagnetic and the $\mathbf{E} \times \mathbf{B}$ terms together. Numerical difficulties have been encountered, mostly at or near the X-points and at the core boundary. For example, the current flow patterns in the core, in the pure diamagnetic and pure $\mathbf{E} \times \mathbf{B}$ cases, are almost perpendicular to each other, and thus reaching a proper numerical steady-state equilibrium requires special care in the way the solution is approached and the new physics terms turned on. Particular attention must also be paid to the boundary condition at the core as well as to the rows of cells where the periodic boundary conditions are being applied. At this time, we have not yet obtained fully satisfactory runs with all terms included at full strength.

5. Conclusions

In this paper, we have presented the simulations of a nominal stellarator island divertor using the 2D plasma fluid code B2.5-solps5.0, solving self-consistently for the electric potential. The influence of drifts and currents has been investigated, and numerical issues involved in their code implementation in such plasma geometries have been addressed. Due to the topological peculiarities of the problem, the potential profile is non-trivial

($\phi \neq 3kT$), and can favor large density accumulation in the island and SOL regions for high-recycling conditions. Current loops are also established in the SOL which may connect to the diverted island region. These current loops grow lopsided under the influence of the $\mathbf{E} \times \mathbf{B}$ drift, but are practically destroyed by diamagnetic effects. Concurrently, the island density accumulation is significantly reduced with the inclusion of drift effects. Simulations simultaneously treating both $\mathbf{E} \times \mathbf{B}$ and diamagnetic terms are in progress. Although the scope of this work is limited because of its 2D nature, the overall structure of the electric field is expected to be robust, at least in toroidal locations where divertor plates are present.

References

[1] A. Komori, N. Ohyabu, S. Masuzaki et al., J. Nucl. Mater. 241–243 (1997) 967.
[2] F. Sardei, Y. Feng, P. Grigull et al., J. Nucl. Mater. 241–243 (1997) 135.
[3] G. Herre, R. Schneider, D. Coster et al., J. Nucl. Mater. 241–243 (1997) 941.
[4] V. Rozhansky, S. Voskoboynikov, E. Kovaltsova et al., Contrib. Plasma Phys. 40 (2000) 423.
[5] R. Schneider, D. Coster, B. Braams et al., Contrib. Plasma Phys. 40 (2000) 328.
[6] G. Herre, P. Grigull, R. Schneider, J. Nucl. Mater. 266–269 (1999) 1015.
[7] Y. Feng, G. Herre, P. Grigull et al., Plasma Phys. Control. Fus. 40 (1998) 371.
[8] Y. Feng, F. Sardei, J. Kisslinger, J. Nucl. Mater. 266–269 (1999) 812.
[9] M. Borchardt, J. Riemann, R. Schneider et al., J. Nucl. Mater., these proceedings (PSI-14).
[10] P.C. Stangeby, A.V. Chankin, Phys. Plasmas 2 (1995) 707.
[11] V. Rozhansky, S. Voskoboynikov, E. Kovaltsova et al., Nucl. Fus., in press.